

# The influence of global form on local orientation anisotropies in human visual cortex

Damien J. Mannion<sup>a,b,\*</sup>, J. Scott McDonald<sup>a</sup>, Colin W.G. Clifford<sup>a,b</sup>

<sup>a</sup>*Colour, Form, and Motion Lab, School of Psychology, The University of Sydney, Australia*

<sup>b</sup>*Australian Research Council Centre for Excellence in Vision Science*

---

## Abstract

Perception of the spatial structure of the environment results from visual system processes which integrate local information to produce global percepts. Here, we investigated whether particular global spatial arrangements evoke greater responses in the human visual system, and how such anisotropies relate to those evident in the responses to the local elements that comprise the global form. We presented observers with Glass patterns; images composed of randomly positioned dot pairings (dipoles) spatially arranged to produce a percept of translational or polar global form. We used functional magnetic resonance imaging (fMRI) to infer the magnitude of neural activity within early retinotopic regions of visual cortex (V1, V2, V3, V3A/B, and hV4) while the angular arrangement of the dipoles was modulated over time to sample the range of orientations. For both translational and polar Glass patterns, V1 showed an increased response to vertical dipole orientations and all visual areas showed a bias towards dipole orientations that were radial to the point of fixation. However, areas V1, V2, V3, and hV4 also demonstrated a bias, only present for polar Glass patterns, towards dipole orientations that were tangential to the point of fixation. This enhanced response to tangential orientations within polar form indicates sensitivity to curvature or more global form characteristics as early as primary visual cortex.

*Keywords:* fMRI, V1, orientation, computational neuroimaging, spatial vision

---

The perception of complex spatial form arises from the global integration of local orientation information. Glass patterns (Glass, 1969; Glass and Perez, 1973) are particularly illustrative of this process. Glass patterns are constructed by the placement of numerous paired dots (dipoles) at random positions within an image with the elements of each dipole at a relative orientation that is consistent with the desired global form. Despite the ambiguous local orientation representation, due to the presence of false dot pairings, the observation of Glass patterns evokes a clear percept of oriented structure. To obtain this percept, the visual system appears to spatially pool the noisy local orientation information to produce a coherent representation of global form (Ostwald et al., 2008; Smith et al., 2002, 2007; Wilson and Wilkinson, 1998).

The perceived Glass pattern form is dependent upon the local spatial arrangement of the paired dots that comprise each dipole. This local orientation structure can be considered within separate coordinate systems, which we have termed field-independent and meridian-relative. Field-independent orientation refers to a coordinate convention which is invariant across the visual field, while meridian-relative orientations are specified relative to the local visual field meridian. As shown in Figure 1, Glass patterns in which the dipoles are aligned along a given field-independent orientation produce the percept of translational structure, while a percept of polar structure is evoked by dipoles that are aligned along a given meridian-relative orientation.

Functional magnetic resonance imaging (fMRI) of human visual cortex has shown that the magnitude of the blood-oxygen level dependent (BOLD) signal is modulated by the local orientation structure; the responses are anisotropic (Clifford et al., 2009; Furmanski and Engel, 2000; Sasaki et al., 2006; Swisher et al., 2010). Here, we investigated whether anisotropies in the response to local Glass pattern orientation structure are affected by the presence of global form. We used fMRI to measure the BOLD signal during the observation of translational and polar Glass patterns which modulated in orientation. We also used a rotating wedge stimulus to define the early retinotopic regions V1, V2, V3, V3A/B, and hV4 and to subdivide each region into a set of preferred visual field meridians. The combination of these measures allowed us to estimate the magnitude of response to local field-independent and meridian-relative orientation from both translational and polar Glass patterns, and hence to infer the influence of global form on local orientation anisotropies.

## Materials and Methods

### Subjects

Four experienced psychophysical observers participated in the current study. Each subject had received a recent optometric examination and all subjects, including those with clinically normal vision, wore customised corrective goggles during the experiment. Subjects gave their informed consent and the protocol was approved by a local ethics committee.

---

\*Corresponding author

Email address: damienm@psych.usyd.edu.au (Damien J. Mannion)

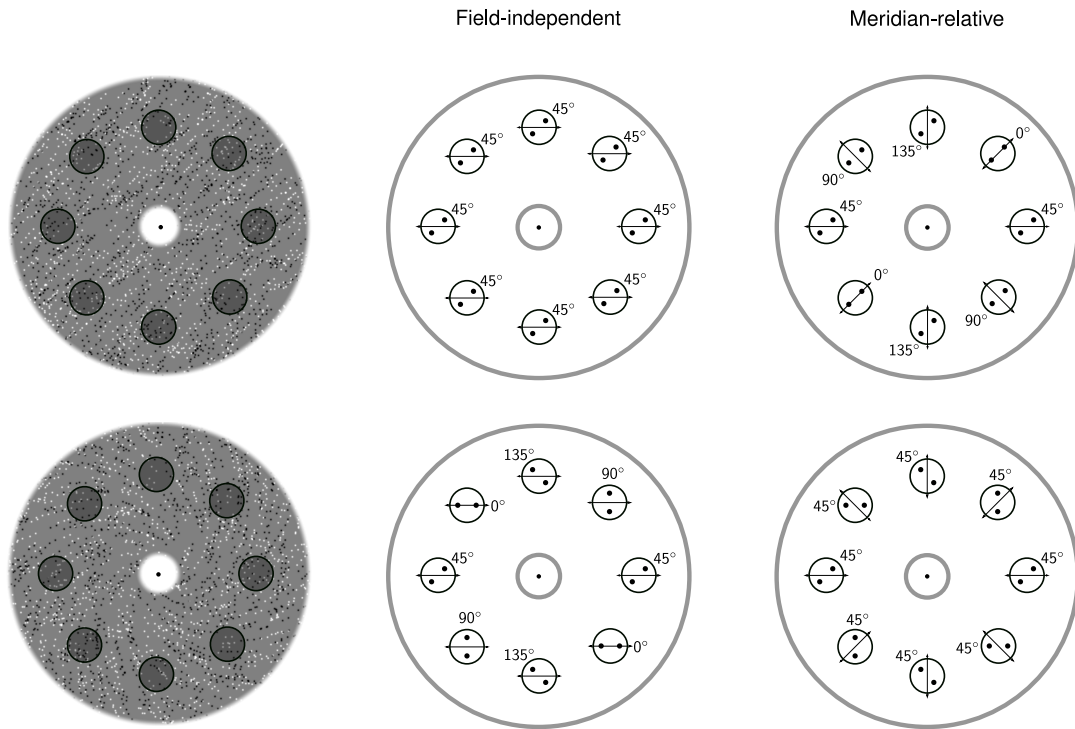


Figure 1: Illustration of translational and polar Glass patterns and their relationships to field-independent and meridian-relative orientation. Translational (upper row) and polar (lower row) Glass patterns are created by transforming a random field of dots along a given field-independent (translational) or meridian-relative (polar) orientation ( $45^\circ$  in this example). The field-independent orientation coordinate system is invariant across the visual field, with  $0^\circ$  as horizontal,  $45^\circ$  as right-tilted oblique,  $90^\circ$  as vertical, and  $135^\circ$  as left-tilted oblique. The dipoles in each of the example visual field locations have a common field-independent orientation in translational Glass patterns and varying field-independent orientation in polar Glass patterns. The meridian-relative orientation coordinate system is rotated to align with the local visual field meridian, with  $0^\circ$  as radial and  $90^\circ$  as tangential. The dipoles in each of the example visual field locations have varying meridian-relative orientations in translational Glass patterns and a common meridian-relative orientation in polar Glass patterns.

### Apparatus

A Philips 3T scanner with a whole-head coil was used to conduct the MRI. Scanning was conducted at two locations—St. Vincent’s Hospital (StV) and the Prince of Wales Medical Research Institute (POWMRI). Functional images were collected using a  $T_2^*$  sensitive, boustrophedon, field-echo echoplanar imaging pulse sequence (TR = 3s, TE = 32ms, flip angle =  $90^\circ$ , FOV =  $69 \times 192 \times 192$ mm, matrix =  $128 \times 128$ , voxel size = 1.5mm isotropic). Images were acquired in 46 ascending interleaved slices in a tilted coronal plane covering the occipital lobes. Anatomical images were collected using a turbo field-echo protocol and consisted of whole-head scans in the axial and sagittal planes (voxel size = 1mm isotropic) and a high resolution partial-head coronal scan (voxel size = 0.75mm isotropic) to recover maximum detail in the occipital lobes.

Stimuli were displayed either by projection onto a screen (StV; 5100MP, Dell Inc., Round Rock, TX) or via a LCD monitor (POWMRI; Philips Healthcare, Best, The Netherlands) positioned behind the bore, each with a spatial resolution of  $1024 \times 768$  pixels and temporal resolution of 60Hz. The display luminance was linearised via spline interpolation (StV) or gamma correction (POWMRI) of values measured with a SpectraScan PR-655 spectrophotometer (Photo Research Inc., Chatsworth,

CA), and had a mean luminance of  $275 \text{ cd/m}^2$  (StV) or  $37 \text{ cd/m}^2$  (POWMRI). Subjects viewed the screen from a distance of 167cm (StV) or 158cm (POWMRI) via a mirror mounted on the head coil, giving a viewing angle of  $19.0^\circ \times 14.3^\circ$  (StV) or  $12.6^\circ \times 9.5^\circ$  (POWMRI). Stimuli were presented using PsychToolbox 3.0.8 (Brainard, 1997; Pelli, 1997). Behavioural responses were indicated via a LU400-PAIR response pad (Cedrus Corporation, San Pedro, CA). Analyses were performed using SPM5 (<http://www.fil.ion.ucl.ac.uk/spm>), mrVista (<http://white.stanford.edu/software>), and custom routines on Matlab 7.8 (The Mathworks, Natick, MA).

### Stimuli

The construction of each Glass pattern began by assigning a random position in the image as the base for each dipole, based on a uniform allocation over area. Dot pairs were then placed equidistant from each base with an inter-dot distance of  $0.3^\circ$  (StV) or  $0.2^\circ$  (POWMRI). The rule governing the dot pair arrangement was dependent upon the pattern type and angle; as shown in Figure 1, translational patterns were formed by aligning the dot pairs along the desired field-independent orientation axis while polar patterns were formed by aligning the dot pairs along the desired meridian-relative orientation axis. Each dot

had a Gaussian profile ( $\sigma$ : 0.03° [StV], 0.02° [POWMRI]) and each dot pair was randomly assigned to be either a full contrast (> 95%) increment or decrement from the background, with the paired dots always having the same polarity. The stimuli were presented within an annulus (inner radius: 0.75° [StV], 0.49° [POWMRI]; outer radius: 7.2° [StV], 4.75° [POWMRI]; raised cosine window at inner and outer edges: 0.35° [StV], 0.24° [POWMRI]) on a background equal to the mean display luminance. Sample Glass pattern stimuli are shown in Supplementary Movies 1 (translational) and 2 (polar).

Visual field polar angles were defined using a wedge that opened 45°, composed of three 15° full contrast radial checkerboard strips, and extended to 7.2° eccentricity (Larsson and Heeger, 2006). The phase of each strip was incremented or decremented by 10° each frame, with the central strip moving in the opposite direction to its flankers. The wedge was presented on a background of mean luminance that was overlaid with a grid of several isopolar and isoeccentric lines to promote stable fixation (Hansen et al., 2007; Schira et al., 2007).

A coordinate convention was adopted for the polar wedge stimuli in which 0° was located at the right horizontal section of the visual field and increasing angles advanced anti-clockwise. An analogous convention was applied for translational (0° = horizontal, 45° = right-tilted oblique, 90° = vertical, 135° = left-tilted oblique) and polar (0° = radial, 45° = anti-clockwise spiral, 90° = concentric, 135° = clockwise spiral) Glass pattern orientation

A small fixation marker was displayed at the centre of the screen throughout stimulus presentation, composed of an outer black circle and an inner circle that was either grey or white.

### *Design*

We used continuous presentation paradigms to measure the BOLD response to modulations in Glass pattern orientation (Yacoub et al., 2008) and visual field polar angle (DeYoe et al., 1996; Engel et al., 1997; Sereno et al., 1995).

Each subject completed at least six runs each of translational and polar Glass pattern presentations. The runs were spread over two scanning sessions, one at POWMRI and one at StV, with each session lasting approximately 70 minutes and consisting of both translational and polar Glass pattern runs.

During each run, the pattern orientation changed with each volume acquisition (3s) in stepwise 11.25° shifts (see Supplementary Movies 1 and 2). The direction of change alternated over runs, with each subject completing an equal number of translational and polar Glass pattern runs in which the direction of change was anti-clockwise and clockwise. The stimulus was absent in the first and last 500ms of each volume to prevent transients induced by abrupt changes in orientation, and a new Glass pattern instance was presented at 1Hz. A full orientation cycle was presented in 48 seconds (16 volumes), and eight complete cycles were completed in each run.

Each subject completed four visual field polar angle runs, in a separate scanning session to the pattern orientation scanning sessions, during which the polar angle of the wedge changed every 1.5s in stepwise 15° shifts. The direction of change alternated between clockwise and anti-clockwise over runs. The

direction of motion in the wedge strips were assigned randomly at the beginning of each volume. A full polar wedge cycle was presented in 36 seconds (12 volumes), and 10 complete cycles were completed in each run.

To control fixation and attention, subjects performed a behavioural task throughout all runs in which they responded to increments and decrements in the luminance of the central fixation dot.

### *Data pre-processing*

Using SPM5, functional images were: corrected for differences in slice acquisition time with the middle slice as reference; corrected for between and within run subject movement; and resliced using 4th degree B-spline interpolation. After discarding the first half-cycle of each run, a correction of +2 volumes (6s) was applied to compensate for the lag in the haemodynamic response. Timecourses from runs in which the stimulus advanced clockwise were temporally reversed, and were then combined with anti-clockwise runs to produce mean timecourses for translational Glass pattern orientation, polar Glass pattern orientation, and visual field polar angle.

A mean anatomical image was formed for each subject by combining the axial and sagittal whole-head scans and the coronal partial head scan. Before averaging, each anatomical image was inhomogeneity corrected (Manjòn et al., 2007), coregistered, and resampled to a voxel resolution of 0.75mm (isotropic) where necessary. Each subject's mean anatomical was then segmented using the automatic routines of mrGray (Teo et al., 1997) and ITKGray (Yushkevich et al., 2006, <http://white.stanford.edu/software>) followed by careful hand editing.

### *Analysis*

The responses to the polar wedge stimulus were used to define the visual areas in early retinotopic cortex. Using mrVista, the preferred visual field polar angle of each voxel was estimated as the phase of the best-fitting sinusoid at the cycle frequency. The inplane voxels were then transformed onto a flattened representation of the cortical surface and the map of angular preferences was used to manually define areas V1, V2, V3, V3A/B, and hV4 based on the nomenclature and criteria of Larsson and Heeger (2006) and Wandell et al. (2007). To support appropriate area definition, eccentricity maps from previous studies with common subjects (Mannion et al., 2009) were also consulted. To restrict visual area definitions to stimulated portions of the visual field, voxels of low coherence (< 0.1) to the polar wedge stimulus and those within the fovea were excluded from further analysis.

The response to the translational and polar Glass pattern orientation stimulus cycles were calculated for each voxel within the identified visual areas. The pattern orientation timecourses were normalised by subtracting and then dividing by the mean voxel response, high-pass filtered (128s cutoff), and averaged over the eight cycles. For each Glass pattern type (translational and polar) and voxel, this produced a 16-item vector of the evoked response to pattern orientation in 11.25° increments

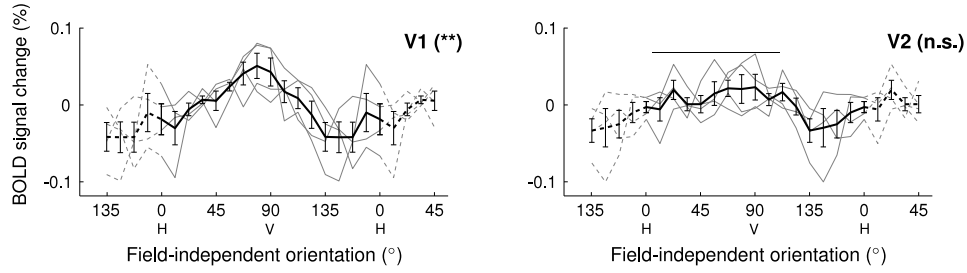


Figure 2: Modulation in V1 (left) and, for comparison, V2 (right) BOLD response to field-independent orientation (averaged over Glass pattern type and meridian-relative orientation), where  $0^\circ$  = horizontal [H],  $45^\circ$  = rightwards tilt,  $90^\circ$  = vertical [V], and  $135^\circ$  = leftwards tilt. The profile is significantly anisotropic in V1 (\*\*;  $p < .01$ ) while no significant anisotropy is present in the profile of V2 (n.s.;  $p > .05$ ). The plot shows mean over subjects  $\pm$  SEM (thick black line) and individual subjects (thin grey lines) and has an extra quarter cycle wrapped at each end (dashed segments).

along the  $[0^\circ, 180^\circ]$  interval. Voxels with a maximum signal change greater than 2 standard deviations above the mean maximum signal change for a given visual area were discarded from further analysis.

The voxels within each visual area were then binned according to their preferred spatial meridian (calculated by wrapping the preferred visual field polar angle at  $180^\circ$ ), with bin centres corresponding to the 16 pattern orientations. The Glass pattern orientation response vectors were then averaged across those voxels within a given visual area with a common spatial polar meridian bin. The data for each subject, visual area, and Glass pattern type thus formed a  $16 \times 16$  matrix (Glass pattern orientation  $\times$  visual field polar meridian). Finally, the data matrices were sheared to transform the dimension indexing the visual field polar meridian to index the circular distance between the Glass pattern orientation and the visual field polar meridian. When applied to the translational Glass pattern matrix (shear slope = +1), this operation transformed the dimension to index meridian-relative orientation, whereas the application to polar Glass pattern matrix (shear slope = -1) transformed the dimension to index field-independent orientation (see Supplementary Figure 1).

A three-way repeated measures ANOVA was conducted for each visual area with subjects as a random factor and Glass pattern type (2 levels; translational, polar), field-independent orientation (16 levels) and meridian-relative orientation (16 levels) as fixed factors. Violations of the assumption of sphericity were corrected by using Huynh-Feldt values in assessing statistical significance.

## Results

We presented observers with translational and polar Glass pattern stimuli modulating in orientation while using fMRI to measure the BOLD response from the early retinotopic areas of visual cortex. We also measured the preferred angular position in the visual field of each voxel, which allowed us to derive profiles of response magnitude to both field-independent and meridian-relative orientation from both translational and polar Glass patterns. We investigated potential anisotropies by performing a three-way repeated measures ANOVA (Glass pattern

type  $\times$  field-independent orientation  $\times$  meridian-relative orientation) on the measured BOLD responses from each of the retinotopic regions V1, V2, V3, V3A/B, and hV4.

There was a significant anisotropy in the measured response profile to field-independent orientation in V1 ( $F_{12,6,37.8} = 3.14$ ,  $p = .003$ ), while there were no significant field-independent anisotropies in V2, V3, V3A/B, or hV4 nor were there significant interactions between field-independent orientation and Glass pattern type or meridian-relative orientation in any area (all  $p > .05$ ). As shown in Figure 2, the response to field-independent orientation (averaged over Glass pattern type and meridian-relative orientation) was maximal around vertical ( $90^\circ$ ) in V1.

The profile of response magnitude to meridian-relative orientation was significantly anisotropic in all areas (V1:  $F_{4,9,14.7} = 5.05$ ,  $p = .007$ ; V2:  $F_{7,1,21.4} = 7.96$ ,  $p < .001$ ; V3:  $F_{7,8,23.5} = 6.36$ ,  $p < .001$ ; V3A/B:  $F_{15,0,45.0} = 3.10$ ,  $p = .002$ ; hV4:  $F_{8,3,25.0} = 6.73$ ,  $p < .001$ ). There was also a significant interaction between meridian-relative orientation and Glass pattern type (translational or polar) in areas V1 ( $F_{15,0,45.0} = 3.98$ ,  $p < .001$ ), V2 ( $F_{6,4,19.1} = 4.71$ ,  $p = .004$ ), V3 ( $F_{8,4,25.1} = 3.93$ ,  $p = .004$ ), and hV4 ( $F_{15,0,45.0} = 6.27$ ,  $p < .001$ ), which was not evident in V3A/B ( $F_{15,0,45.0} = 0.87$ ,  $p = .605$ ). As shown in Figure 3, the response to meridian-relative orientation defined within a translational Glass pattern showed a unimodal profile of anisotropy in all areas, with a peaked response to radial orientations. However, when defined within a polar Glass pattern, the profile of anisotropy was bimodal in V1, V2, V3, and hV4, with peaks at both radial and tangential orientations.

## Discussion

We investigated the representation of the orientation structure of complex spatial form within human visual cortex. Using fMRI, we measured the BOLD response from the early retinotopic regions V1, V2, V3, V3A/B and hV4 during the observation of translational and polar Glass patterns which modulated in orientation. By interpreting the measured responses with regards to the preferred visual field location of each voxel, derived from rotating wedge retinotopic mapping procedures, we obtained distributions of response magnitude to field-independent

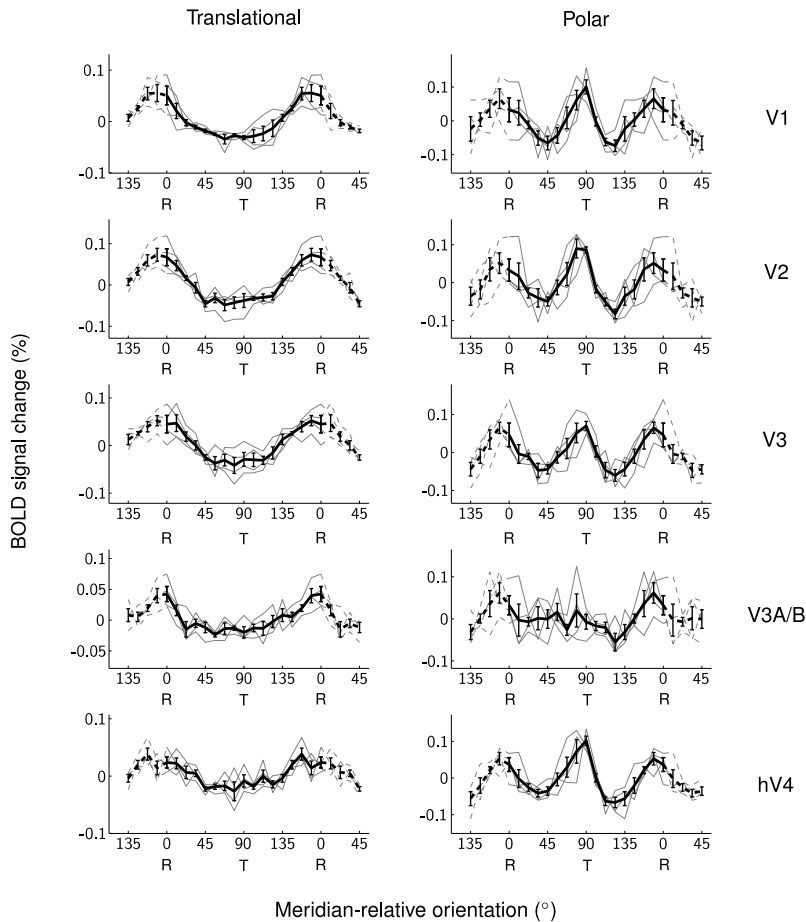


Figure 3: Modulation in BOLD response across each of the early visual areas to meridian-relative orientations defined within translational (left) and polar (right) Glass patterns, where  $0^\circ$  = radial [R] and  $90^\circ$  = tangential [T]. All plots show mean over subjects  $\pm$  SEM (thick black line) and individual subjects (thin grey lines), have an extra quarter cycle wrapped at each end (dashed segments), and are presented on ordinate scales that are unstandardised across plots.

and meridian-relative orientation from both translational and polar Glass patterns. We examined how anisotropies in the magnitude of response to field-independent and meridian-relative orientation are affected by the presence of global spatial structure.

An anisotropy in the measured BOLD response to field-independent orientation was only present in V1, where a greater response to field-independent orientations near vertical was observed. Jenkins (1985) reported that the perception of spatial form can be obtained with greater dot pair separation in vertical translational Glass patterns than those at horizontal or oblique orientations, and suggested that vertical receptive fields at the level of local orientation extraction may be elongated relative to those at horizontal and obliques. Our observed pattern of anisotropy is broadly consistent with this notion, and suggests that the source of the behavioural anisotropy may be located within, and perhaps not propagated beyond, primary visual cortex. However, we did not observe any evidence of a correlate of the enhanced psychophysical sensitivity to oblique translational Glass patterns reported by Wilson et al. (2001).

We report a striking difference in the profile of responses to

meridian-relative orientations defined within polar Glass patterns relative to those within translational Glass patterns. The anisotropic response to meridian-relative orientation within translational patterns is characterised by a preference for radial orientations, with decreased levels of activity with increasing angular distance from the radial meridian-relative orientation evident in all areas (V1, V3, V3, V3A/B, and hV4). This preference for radial meridian-relative orientations is also evident when defined within polar Glass pattern form, and is consistent with previous reports of a radial bias (Clifford et al., 2009; Sasaki et al., 2006). However, it is accompanied for polar Glass patterns by an additional response peak to tangential meridian-relative orientations in areas V1, V2, V3, and hV4 such that the meridian-relative orientation which evoked the lowest response when defined within translational Glass patterns evoked the highest response when defined within polar Glass patterns.

While the orientation structure of translational and polar Glass patterns is similar when considered over localised regions of space (Smith et al., 2002; Wilson and Wilkinson, 1998), spatially extended analysis yields differences between the two pattern types. The common meridian-relative orientation of

the dipoles in a given polar Glass pattern combines over space to form higher-order structure—radial integrates to starbursts, oblique to spirals, and tangential to concentric circles. Hence, differences in the profile of meridian-relative anisotropy derived from translational relative to those from polar Glass patterns are likely due to the influence of mechanisms sensitive to aspects of spatial form beyond the local orientation structure such as curvature or global shape.

We find a clear difference between responses to tangential meridian-relative orientations defined within translational and polar Glass patterns. This may reflect either enhanced sensitivity to the higher-order form present in tangential polar Glass patterns (circles) or enhanced sensitivity to the mid-level spatial structure of which such global shape is composed (curvature). Smooth, closed contours such as circles are common in the natural environment (Chow et al., 2002; Geisler et al., 2001; Sigman et al., 2001) and may be of sufficient ecological importance to merit an enhanced neural response. Accordingly, humans show fine behavioural sensitivity (Achtman et al., 2003; Kurki and Saarinen, 2004; Seu and Ferrera, 2001; Wilson et al., 1997; Wilson and Wilkinson, 1998) and increased fMRI response (Ban et al., 2006; Dumoulin and Hess, 2007; Wilkinson et al., 2000) when the visual image contains circular orientation structure.

We find that the meridian-relative anisotropy from both translational and polar Glass patterns shows a preference for radial orientations. While comparisons of absolute response magnitude between translational and polar Glass patterns are not meaningful in the current study, it raises the possibility that the visual system may not have a preferential response to global starburst structure beyond a preference for its constituent radial elements. Future neuroimaging and behavioural investigations in which polar Glass patterns are centred away from fixation, and thus more balanced in their meridian-relative orientation composition, may clarify this relationship.

We observed a preference for tangential meridian-relative orientations defined within polar Glass patterns in the fMRI BOLD response as early as V1. While this is consistent with previous fMRI reports of early cortical modulation by global shape (Altmann et al., 2003; Ban et al., 2006; Kourtzi et al., 2003), it is inconsistent with electrophysiological recordings from macaque V2 that show comparable responses to translational, starburst, and circular Glass patterns (Smith et al., 2007). We speculate that this inconsistency may be due to the influence of anaesthesia on the macaque neural responses, as noted by Smith et al. (2007), or may reflect the imperfect correlation between the fMRI BOLD response and spiking activity (Logothetis, 2008). In particular, the BOLD response is especially sensitive to feedback signals (Logothetis and Wandell, 2004), which suggests that the observed modulation in early visual cortex may reflect the influences of higher visual areas (Ban et al., 2006).

Visual area hV4 has been accorded a primary role in the perception of spatial form, and is a likely source of modulatory feedback to earlier visual areas. Macaque V4 possesses neurons selective for extended contours such as starbursts, spirals, and concentric circles (David et al., 2006; Gallant et al., 1996),

and hV4 shows enhanced fMRI responses to starburst and circular gratings (Wilkinson et al., 2000) and to circular structure beyond mid-level curvature (Dumoulin and Hess, 2007). Computational models of Glass pattern perception have identified hV4 as displaying global shape selectivity by pooling local orientation signals extracted by earlier visual areas (Wilson et al., 1997; Wilson and Wilkinson, 1998), and the perception of starburst and concentric structure in Glass patterns has been shown to be impaired in a patient with a lesion in the vicinity of hV4 (Gallant et al., 2000). Furthermore, the finding in the current study that the dorsal area V3A/B does not show enhanced sensitivity for tangential meridian-relative orientations in the context of polar Glass patterns is consistent with the identification of hV4 and the ventral stream as the pathway mediating shape perception.

## Acknowledgments

We thank the radiography teams at St. Vincent's Hospital and the Prince of Wales Medical Research Institute for assistance with data acquisition. This work was supported by an Australian Postgraduate Award to DM, an Australian Research Fellowship to CC, and by grants from the Australian Research Council and the National Health and Medical Research Council.

## References

- Achtman, R. L., Hess, R. F., Wang, Y.-Z., 2003. Sensitivity for global shape detection. *J Vis* 3 (10), 616–624.
- Altmann, C. F., Bühlhoff, H. H., Kourtzi, Z., 2003. Perceptual organization of local elements into global shapes in the human visual cortex. *Curr Biol* 13 (4), 342–349.
- Ban, H., Yamamoto, H., Fukunaga, M., Nakagoshi, A., Umeda, M., Tanaka, C., Ejima, Y., 2006. Toward a common circle: interhemispheric contextual modulation in human early visual areas. *J Neurosci* 26 (34), 8804–8809.
- Brainard, D. H., 1997. The psychophysics toolbox. *Spat Vis* 10 (4), 433–436.
- Chow, C. C., Jin, D. Z., Treves, A., 2002. Is the world full of circles? *J Vis* 2 (8), 571–576.
- Clifford, C. W., Mannion, D. J., McDonald, J. S., 2009. Radial biases in the processing of motion and motion-defined contours by human visual cortex. *J Neurophysiol* 102 (5), 2974–2981.
- David, S. V., Hayden, B. Y., Gallant, J. L., 2006. Spectral receptive field properties explain shape selectivity in area V4. *J Neurophysiol* 96 (6), 3492–3505.
- DeYoe, E. A., Carman, G. J., Bandettini, P., Glickman, S., Wieser, J., Cox, R., Miller, D., Neitz, J., 1996. Mapping striate and extrastriate visual areas in human cerebral cortex. *Proc Natl Acad Sci USA* 93 (6), 2382–2386.
- Dumoulin, S. O., Hess, R. F., 2007. Cortical specialization for concentric shape processing. *Vision Res* 47 (12), 1608–1613.
- Engel, S. A., Glover, G. H., Wandell, B. A., 1997. Retinotopic organization in human visual cortex and the spatial precision of functional MRI. *Cereb Cortex* 7 (2), 181–192.
- Furmanski, C. S., Engel, S. A., 2000. An oblique effect in human primary visual cortex. *Nat Neurosci* 3 (6), 535–536.
- Gallant, J. L., Connor, C. E., Rakshit, S., Lewis, J. W., Van Essen, D. C., 1996. Neural responses to polar, hyperbolic, and Cartesian gratings in area V4 of the macaque monkey. *J Neurophysiol* 76 (4), 2718–2739.
- Gallant, J. L., Shoup, R. E., Mazer, J. A., 2000. A human extrastriate area functionally homologous to macaque V4. *Neuron* 27 (2), 227–235.
- Geisler, W. S., Perry, J. S., Super, B. J., Gallogly, D. P., 2001. Edge co-occurrence in natural images predicts contour grouping performance. *Vision Res* 41 (6), 711–724.
- Glass, L., 1969. Moiré effect from random dots. *Nature* 223 (5206), 578–580.

- Glass, L., Perez, R., 1973. Perception of random dot interference patterns. *Nature* 246 (5432), 360–362.
- Hansen, K. A., Kay, K. N., Gallant, J. L., 2007. Topographic organization in and near human visual area V4. *J Neurosci* 27 (44), 11896–11911.
- Jenkins, B., 1985. Orientational anisotropy in the human visual system. *Percept Psychophys* 37 (2), 125–134.
- Kourtzi, Z., Tolias, A. S., Altmann, C. F., Augath, M., Logothetis, N. K., 2003. Integration of local features into global shapes: monkey and human fMRI studies. *Neuron* 37 (2), 333–346.
- Kurki, I., Saarinen, J., 2004. Shape perception in human vision: specialized detectors for concentric spatial structures? *Neurosci Lett* 360 (1-2), 100–102.
- Larsson, J., Heeger, D. J., 2006. Two retinotopic visual areas in human lateral occipital cortex. *J Neurosci* 26 (51), 13128–13142.
- Logothetis, N. K., 2008. What we can do and what we cannot do with fMRI. *Nature* 453 (7197), 869–878.
- Logothetis, N. K., Wandell, B. A., 2004. Interpreting the BOLD signal. *Annu. Rev. Physiol.* 66, 735–769.
- Manjòn, J. V., Lull, J. J., Carbonell-Caballero, J., Garca-Martí, G., Martí-Bonmati, L., Robles, M., 2007. A nonparametric MRI inhomogeneity correction method. *Med Image Anal* 11 (4), 336–345.
- Mannion, D. J., McDonald, J. S., Clifford, C. W. G., 2009. Discrimination of the local orientation structure of spiral Glass patterns early in human visual cortex. *NeuroImage* 46 (2), 511–515.
- Ostwald, D., Lam, J. M., Li, S., Kourtzi, Z., 2008. Neural coding of global form in the human visual cortex. *J Neurophysiol* 99 (5), 2456–2469.
- Pelli, D. G., 1997. The VideoToolbox software for visual psychophysics: transforming numbers into movies. *Spat Vis* 10 (4), 437–442.
- Sasaki, Y., Rajimehr, R., Kim, B. W., Ekstrom, L. B., Vanduffel, W., Tootell, R. B., 2006. The radial bias: a different slant on visual orientation sensitivity in human and nonhuman primates. *Neuron* 51 (5), 661–670.
- Schira, M. M., Wade, A. R., Tyler, C. W., 2007. Two-dimensional mapping of the central and parafoveal visual field to human visual cortex. *J Neurophysiol* 97 (6), 4284–4295.
- Sereno, M. I., Dale, A. M., Reppas, J. B., Kwong, K. K., Belliveau, J. W., Brady, T. J., Rosen, B. R., Tootell, R. B., 1995. Borders of multiple visual areas in humans revealed by functional magnetic resonance imaging. *Science* 268 (5212), 889–893.
- Seu, L., Ferrera, V. P., 2001. Detection thresholds for spiral Glass patterns. *Vision Res* 41 (28), 3785–3790.
- Sigman, M., Cecchi, G. A., Gilbert, C. D., Magnasco, M. O., 2001. On a common circle: natural scenes and Gestalt rules. *Proc Natl Acad Sci USA* 98 (4), 1935–1940.
- Smith, M. A., Bair, W., Movshon, J. A., 2002. Signals in macaque striate cortical neurons that support the perception of Glass patterns. *J Neurosci* 22 (18), 8334–8345.
- Smith, M. A., Kohn, A., Movshon, J. A., 2007. Glass pattern responses in macaque V2 neurons. *J Vis* 7 (3), 1–15.
- Swisher, J. D., Gatenby, J. C., Gore, J. C., Wolfe, B. A., Moon, C.-H., Kim, S.-G., Tong, F., 2010. Multiscale pattern analysis of orientation-selective activity in the primary visual cortex. *J Neurosci* 30 (1), 325–330.
- Teo, P. C., Sapiro, G., Wandell, B. A., 1997. Creating connected representations of cortical gray matter for functional MRI visualization. *IEEE Trans Med Imaging* 16 (6), 852–863.
- Wandell, B. A., Dumoulin, S. O., Brewer, A. A., 2007. Visual field maps in human cortex. *Neuron* 56 (2), 366–383.
- Wilkinson, F., James, T. W., Wilson, H. R., Gati, J. S., Menon, R. S., Goodale, M. A., 2000. An fMRI study of the selective activation of human extrastriate form vision areas by radial and concentric gratings. *Curr Biol* 10 (22), 1455–1458.
- Wilson, H. R., Loffler, G., Wilkinson, F., Thistlethwaite, W. A., 2001. An inverse oblique effect in human vision. *Vision Res* 41 (14), 1749–1753.
- Wilson, H. R., Wilkinson, F., 1998. Detection of global structure in Glass patterns: implications for form vision. *Vision Res* 38 (19), 2933–2947.
- Wilson, H. R., Wilkinson, F., Asaad, W., 1997. Concentric orientation summation in human form vision. *Vision Res* 37 (17), 2325–2330.
- Yacoub, E., Harel, N., Ugurbil, K., 2008. High-field fMRI unveils orientation columns in humans. *Proc Natl Acad Sci USA* 105 (30), 10607–10612.
- Yushkevich, P. A., Piven, J., Hazlett, H. C., Smith, R. G., Ho, S., Gee, J. C., Gerig, G., 2006. User-guided 3D active contour segmentation of anatomical structures: significantly improved efficiency and reliability. *NeuroImage* 31 (3), 1116–1128.